

Radio and X-ray observations of the intermittent pulsar J1832+0029

D.R. Lorimer^{1,2}, A.G. Lyne³, M.A. McLaughlin^{1,2}, M. Kramer^{3,4}, G.G. Pavlov^{5,6}, and
C. Chang⁵

ABSTRACT

We report on radio and X-ray observations of PSR J1832+0029, a 533-ms radio pulsar discovered in the Parkes Multibeam Pulsar Survey. From radio observations taken with the Parkes, Lovell and Arecibo telescopes, we show that this pulsar exhibits two spindown states akin to PSRs B1931+24 reported by Kramer et al. and J1841–0500 reported by Camilo et al. Unlike PSR B1931+24, which switches between “on” and “off” states on a 30–40 day time-scale, PSR J1832+0029 is similar to PSR J1841–0500 in that it spends a much longer period of time in the off-state. So far, we have fully sampled two off-states. The first one lasted between 560 and 640 days and the second one lasted between 810 and 835 days. From our radio timing observations, the ratio of on/off spindown rates is 1.77 ± 0.03 . *Chandra* observations carried out during both the on- and off-states of this pulsar failed to detect any emission. Our results challenge but do not rule out models involving accretion onto the neutron star from a low-mass stellar companion. In spite of the small number of intermittent pulsars currently known, difficulties in discovering them and in quantifying their behavior imply that their total population could be substantial.

Subject headings: pulsars: individual (PSR B1931+24; PSR J1832+0029; PSR J1841–0500)

¹Department of Physics, West Virginia University, White Hall, Morgantown, WV 26506

²National Radio Astronomy Observatory, Green Bank, WV 24944

³Jodrell Bank Centre for Astrophysics, The University of Manchester, Alan Turing Building, Manchester M13 9PL, UK

⁴Max-Planck-Institut für Radioastronomie, Auf dem Hügel 69, 53121 Bonn, Germany

⁵Department of Astronomy and Astrophysics, The Pennsylvania State University, 525 Davey Lab., University Park, PA 16802

⁶St.-Petersburg State Polytechnical University, Polytekhnicheskaya ul. 29, St.-Petersburg 195251, Russia

1. Introduction

It is well established that not all radio pulsars emit radiation during each rotation. Backer (1970) first observed this phenomenon and demonstrated that some pulsars exist in a “null state” for several pulse periods before switching back on again. Pulsar nulling has been investigated extensively over the years (e.g., Ritchings 1976; Rankin 1986; Biggs 1992). From a study of pulsars in the Parkes Multibeam Pulsar Survey (PMPS; Manchester et al. 2001), Wang et al. (2007) confirmed earlier evidence (Ritchings 1976) that the fraction of nulling pulses generally increases with increasing characteristic age.

In addition to the nulling phenomenon, it has become apparent that a new class of intermittent pulsars exist where no radiation is observed over much longer time-scales. In a single-pulse analysis of archival PMPS data, McLaughlin et al. (2006) discovered a new class of neutron stars (Rotating Radio Transients) from which radio emission is detectable, on average, only 1 s per day in an apparently random fashion. In the same year, Kramer et al. (2006) reported the discovery of a more deterministic type of intermittency in PSR B1931+24, which appears to be the prototype of a large population of pulsars that have so far been difficult to detect. As Kramer et al. demonstrated, PSR B1931+24 shows a quasi-periodic on/off cycle with a period of 30–40 days in which the spindown rate increases by $\sim 50\%$ when the pulsar is in its on-state compared to the off-state. In this paper, we report observations characterizing intermittent behavior in PSR J1832+0029 an apparently ordinary 533-ms pulsar with a characteristic age of 5.6 Myr which was discovered as part of the PMPS (Lorimer et al. 2006). Earlier accounts of this work we presented by Kramer (2008) and Lyne (2009). Very recently, Camilo et al. (2012) announced the discovery of PSR J1841–0500, a 912-ms pulsar which has so far shown one off-state lasting 580 days. Like B1931+24, the spindown rate in the on-state is higher than the off-state. For J1841–0500 the increase is approximately 150%! These pulsars are dramatic examples of a newly recognized and large group of pulsars which show changes in their emission properties and period derivatives (Lyne et al. 2010) which are correlated and often quasi-periodic. Understanding pulsar intermittency will shed new insights into neutron star physics and populations.

The long off-states of intermittent pulsars are in stark contrast to the longest known quiescence times of nulling pulsars, i.e. they exceed the typical nulling time scale by about five orders of magnitude. In addition, the observed increase in spindown rate points to a significant increase in the magnetospheric particle outflow when the pulsar switches on, indicating that a pulsar wind plays a significant role in neutron star spin evolution. As described by Kramer et al. (2006), and discussed later in this paper, the spindown rate changes allow us to estimate the current density associated with the radio emission.

The difficulties in detecting and identifying intermittent pulsars imply that the few

we currently observe represent a potentially substantial population of similar objects in the Galaxy. To better understand this population, it is therefore important to establish the related time-scales for the non-emitting state. Here we detail our observations of intermittent behavior in PSR J1832+0029. In §2 we describe the radio observations we have carried out to characterize its intermittency. In §3 we describe the *Chandra* X-ray observations which constrain the high-energy emission from the pulsar. In §4, we discuss the implications of our results.

2. Radio observations of PSR J1832+0029

PSR J1832+0029 was first detected during the PMPS in an observation made on 2000 November 23. Following its confirmation observation in 2003 September as part of follow-up observations for the survey (Lorimer et al. 2006), PSR J1832+0029 has been observed regularly by both the Parkes 64-m and Lovell 76-m radio telescopes. Parkes observations span the period from 2004 September until 2008 September. Lovell observations began in 2006 March and continue to be made. To date, a total of 422 individual detections of the pulsar have been collected (331 of these with the Lovell telescope). The initial Parkes observations provided routine detections of the pulsar at 1374 and 1518 MHz in five minute pointings until 2004 May. Despite 27 observations of the pulsar between 2004 June 26 and 2006 January 7, the pulsar was not detected. By 2005 March, the Parkes observation times had increased to 20 minutes. The non-detections mean that the flux density of PSR J1832+0029 must have been less than $70 \mu\text{Jy}$ during the period 2004 May to 2005 February for the 5-minute observations and below $40 \mu\text{Jy}$ for the 20-min observations carried out between 2005 March and 2006 January. The pulsar was finally detected again on 2006 March 3 in a 20-min observation at 1374 MHz. It was subsequently routinely detectable, primarily with the Lovell telescope, until 2010 April 7, after which it became undetectable until 2012 July 20 when it resumed its regular behavior.

In all of the observations in which the pulsar was detected, we find no evidence for any variation in the pulse width (7.1 ms full-width at half maximum) or flux density ($140 \mu\text{Jy}$) as originally presented in Lorimer et al. (2006). Currently our Parkes and Lovell observations provide only modest constraints on the degree of polarization in PSR J1832+0029 and indicate that it is less than 20% linearly polarized. As we discuss later (§4.2), sensitive observations of this pulsar’s polarimetric properties could be valuable in helping to discriminate between various proposed models

To make the most stringent constraints of PSR J1832+0029 during its off-state, on 2011 March 8 and 9 we carried out two 1-hr observations using the 305-m William E. Gordon

Arecibo radio telescope. Both observations were conducted using the L-band wide receiver¹ and the Wideband Arecibo Pulsar Processors (WAPPs; Dowd et al. 2000). Four WAPPs were used to measure three-level autocorrelation functions every 128 μ s in each of four 100-MHz sub-bands spanning 1100–1500 MHz. The data from each WAPP were Fourier transformed using the `filterbank` program within the SIGPROC software package² to synthesize a filterbank with 512 frequency channels, each of width 781.25 kHz. These channelized data were then dedispersed at the pulsar’s dispersion measure (DM) of 28.3 cm^{−3} pc and folded over a range of trial periods around the nominal value predicted by our timing model using SIGPROC’s `fold` program. A blind periodicity search was also carried out using SIGPROC’s `seek` program down to a signal-to-noise ratio (S/N) of 6. PSR J1832+0029 was not detected in either of these analyses. Assuming an average gain of 8.5 K/Jy which is appropriate for the large zenith angles during the observation (17–20 degrees), these S/N limits in the searching and folding analyses translate to an upper limit on the flux of 2–3 μ Jy in each observation. Folding the data coherently across both days also resulted in no detection, with a corresponding upper limit of 1.6 μ Jy. At its nominal on-state flux density of 140 μ Jy, the pulsar would have been detected with S/N of approximately 440. We can therefore constrain any emission in the off-state to be less than one part in 440 of the flux density in the on-state. At the distance $d = 1.3$ kpc inferred from the pulsar’s dispersion measure and the Cordes & Lazio (2002) free electron distribution model, the upper limit on the 1400-MHz luminosity from these observations is 2.7 μ Jy kpc². This limit is a factor of 16 lower than that inferred for the off-state of PSR B1931+24 (Kramer et al. 2006) and an order of magnitude below the faintest pulsar currently known (PSR J2144–3933; Manchester et al. 1996).

3. X-ray observations of PSR J1832+0029

PSR J1832+0029 was observed with the Advanced CCD Imaging Spectrometer (ACIS) on board *Chandra* on 2007 October 19 (observation ID 9145) and 2011 March 28 (observation ID 12256), when the pulsar was in on- and off-states, respectively. In both observations, the target was imaged near the optical axis on the S3 chip in Timed Exposure mode with a frame time of 3.24 s. Other activated chips were I2, I3, S1, S2, and S4. The data were telemetered in Very Faint format, optimal for distinguishing between X-ray events and events associated with cosmic rays. The useful effective exposure times (livetimes) were 19.87 ks and 22.75 ks for the first and second observations, respectively.

¹<http://www.naic.edu/~astro/RXstatus/Lwide/Lwide.shtml>

²<http://sigproc.sourceforge.net>

Inspection of the ACIS images shows no X-ray sources closer than $\approx 20''$ from the pulsar position quoted in Table 1. To accurately place upper limits on the pulsar’s X-ray emission, we attempted to improve absolute astrometry by cross-correlation of the ACIS positions of field X-ray sources with their possible counterparts in the Two Micron All Sky Survey (2MASS) catalog, using the `reproject_aspect` script³. Because of the small number of plausible matches between the X-ray and 2MASS sources (e.g., 6 sources with $< 2''$ separation, within $9'$ from the aim point), the correction turned out to be substantially dependent on the choice of sources. We chose four 2MASS sources with likely X-ray counterparts on the S3 chip (separations $< 1''.2$) for each of the observations, which resulted in $0''.3$ and $0''.2$ corrections in the pulsar’s position for the first and second observations, respectively (i.e., less than the size of the ACIS pixel, $0''.492$). The corrected images are shown in Fig. 1.

We analyzed the data in the ACIS energy range of 0.3–8 keV, conservatively choosing $r = 3''$ circles around the radio pulsar position for the source region, which includes 99% of all source counts, for a typical pulsar spectrum. We measured the background, $N_b = 1140$ and 1062 counts for the first and second observations, respectively, in the $80''$ radius circle around the pulsar position, excluding the $r = 10''$ circle around the pulsar and $r = 5''$ circle around the faint (and variable) field source $\approx 20''$ south of the pulsar (i.e., the area of background aperture is $A_b = 19,713 \text{ arcsec}^2$). With the background surface densities $N_b/A_b = 0.058 \pm 0.002$ and $0.054 \pm 0.002 \text{ counts arcsec}^{-2}$, we expect $n_b = 1.64 \pm 0.05$ and 1.54 ± 0.05 background counts in the $r = 3''$ source apertures for the first and second observations, respectively.

The detected numbers of source and background counts in the source aperture are $n = 0$ and 3, for the first and second observations, respectively (the same as in the uncorrected images). This means that the pulsar was not detected in our observations, and we can only put upper limits on its count rate and flux. Assuming Poisson statistics, the upper limit n_u on the total number of counts in the detection area at confidence level C can be estimated (see, e.g., Gehrels 1986) as follows:

$$C = 1 - \sum_{m=0}^n \frac{n_u^m \exp(-n_u)}{m!}, \quad (1)$$

which leads to the upper limit $n_{s,u} = n_u - n_b$ on the number of source counts. For the first observation ($n = 0$), $n_u = -\ln(1 - C)$ and $n_{s,u} = 2.97$ counts for $C = 0.99$. For the second observation ($n = 3$), the corresponding upper limit for $C = 0.99$ is 10.05 counts (see Table 1 in Gehrels 1986), and $n_{s,u} = 8.51$ counts. The source count rate upper limits at the

³http://cxc.harvard.edu/ciao/threads/reproject_aspect

99% confidence level are therefore $R_{s,u} = 1.5 \times 10^{-4}$ counts s⁻¹ for the first observation and $R_{s,u} = 3.7 \times 10^{-4}$ counts s⁻¹ for the second observation.

4. Discussion

The radio observations reported above suggest long-term intermittent behavior in PSR J1832+0029, while the X-ray observations failed to detect any difference in the high-energy emission between the on- and off-states. We now discuss the implications of these observations.

4.1. Spindown behavior in the two states

To track the variation in spin frequency (ν) of PSR J1832+0029 we used the TEMPO2 software package (Hobbs et al. 2006) and its `stridelfit` plugin to carry out measurements of ν based on timing model fits to short (30-day time span) segments of data in which the position was fixed at the nominal values found by Lorimer et al. (2006) and the spin frequency derivative $\dot{\nu}$ was assumed to be zero. As shown in Fig. 2, this analysis reveals a clear discontinuity in the spindown behavior during the off-states. Two explanations could account for this: (i) the pulsar suffered a period glitch during the off-states; (ii) the spindown rate was different during the off-states, as is observed for PSRs B1931+24 and J1841–0500. Although it is possible to fit across the 2004–2005 period, resulting in $\Delta\nu/\nu = (5.34 \pm 0.07) \times 10^{-8}$ for the putative glitch, no exponential recovery is observed and the abrupt turn-off observed in emission is inconsistent with other observations of glitching pulsars (see, e.g., Espinoza et al. 2011). A similar conclusion can be reached for the 2010–2012 off-state. Henceforth we examine the hypothesis where the spindown rate of PSR J1832+0029 has two distinct values which we refer to as $\dot{\nu}_{\text{on}}$ and $\dot{\nu}_{\text{off}}$.

Using TEMPO2, we obtained independent timing solutions in each of the two on-states. The results of these analyses are summarized in Table 1. The pulsar’s DM was not constrained by these analyses and was therefore held fixed at the value reported by Lorimer et al. (2006; DM = 28.3 cm⁻³ pc). The shorter timing baseline (~ 270 days) for the first on-state compared to the second one (~ 4 yr) means that the timing parameters obtained from it are less precise and subject to covariances. So far, we have only sampled ~ 1 month in the current (third) on-state. To minimize these covariances, we held the position in the first on-state fit fixed at the position derived from the second on-state. While the post-fit residuals for the first on-state are approximately white, a significant amount of timing noise is present in the residuals from the second on-state shown in Fig. 3. This behavior

can be removed by fitting multiple sinusoids to the data (the “harmonic whitening” technique; Hobbs et al. 2004). To check the effect on the measured parameters in Table 1, we carried out such an analysis using the `fitwaves` plugin to TEMPO2. The residuals can be whitened by removing six harmonically related sinusoids and the result fit parameters are all within $1\text{-}\sigma$ of the values presented in Table 1. We therefore adopt the parameters from the second on-state as being our most precise measurements of the pulsar to date and, hence, $\dot{\nu}_{\text{on}} = -(5.44505 \pm 0.00007) \times 10^{-15} \text{ s}^{-2}$.

To measure $\dot{\nu}_{\text{off}}$, we accounted for the uncertainties in off/on switching epochs in the following way. We first assumed that the nominal switch-off epoch (T_{off}) of the pulsar occurred midway between the date of the last detection during the second on-phase ($T_1 = \text{MJD } 55293.33$) and the first non-detection ($T_2 = \text{MJD } 53301.99$). Similarly, for the nominal switch-on epoch (T_{on}), we adopt the midpoint between the last non-detection ($T_3 = \text{MJD } 56110.85$) and the first re-detection of the third on-phase ($T_4 = \text{MJD } 56128.78$). Using TEMPO2, we computed $\nu(T_{\text{off}})$ and $\nu(T_{\text{on}})$ — the nominal pulse frequencies at both T_{off} and T_{on} as predicted by the second and third on-state timing models, respectively. The off-state spindown rate

$$\dot{\nu}_{\text{off}} = \frac{\nu(T_{\text{on}}) - \nu(T_{\text{off}})}{T_{\text{on}} - T_{\text{off}}} = -(3.08 \pm 0.05) \times 10^{-15} \text{ s}^{-2}.$$

Here the uncertainty in $\dot{\nu}_{\text{off}}$ is dominated by the uncertainty in $T_{\text{on}} - T_{\text{off}}$ which we estimated to be the mean of the two time windows of interest here (i.e. $(T_4 - T_3 + T_2 - T_1)/2$). A similar analysis for the first off-state yields $\dot{\nu}_{\text{off}} = -(3.2 \pm 0.2) \times 10^{-15} \text{ s}^{-2}$. These results imply that the ratio of on/off spindown rates $\mathcal{R} = \dot{\nu}_{\text{on}}/\dot{\nu}_{\text{off}}$ is therefore 1.77 ± 0.03 , i.e. slightly higher than PSR B1931+24 but below PSR J1841–0500.

4.2. Charge density in the pulsar magnetosphere

To estimate the implied current flow in the pulsar magnetosphere for both the on and off-states, we follow Kramer et al. (2006) and consider the simplest possible emission model. We assume that, in the off-state, the pulsar spins down by a mechanism that does not involve a substantial particle ejection (e.g., it would be magnetic dipole radiation if the pulsar were in vacuum), while the rate in the on-state is enhanced by a torque from the current of an additional plasma outflow. Assuming that the spindown energy loss rate in the on-state, \dot{E}_{on} , may be written as the sum of the energy loss rate in the off-state, \dot{E}_{off} , and the energy loss due to the additional plasma, \dot{E}_{plasma} , the corresponding charge density (in cgs units) in the plasma

$$\rho_{\text{plasma}} = \frac{3I(\dot{\nu}_{\text{off}} - \dot{\nu}_{\text{on}})}{R_{\text{pc}}^4 B_{\text{off}}}. \quad (2)$$

Here I is the moment of inertia of the neutron star,

$$R_{\text{pc}} = \sqrt{\frac{2\pi\nu R_{\text{NS}}^3}{c}} \quad (3)$$

is the polar cap radius, B_{off} is the dipole surface magnetic field strength calculated from the spin frequency and spindown rate in the off-state, and c is the speed of light. For a canonical neutron star of radius $R_{\text{NS}} = 10^6$ cm and moment of inertia $I = 10^{45}$ gm cm², we find $\rho_{\text{plasma}} \simeq 62$ esu cm⁻³. This is slightly higher than the so-called Goldreich-Julian density

$$\rho_{\text{GJ}} = \frac{B_{\text{off}}}{Pc} \simeq 44 \text{ esu cm}^{-3} \quad (4)$$

which is the charge density required to radiate along the open magnetic field lines in the idealized pulsar magnetosphere model proposed by Goldreich & Julian (1969).

For PSR B1931+24, Kramer et al. (2006) found that $\rho_{\text{GJ}} \simeq \rho_{\text{plasma}} \simeq 100$ esu cm⁻³. Taking the corresponding values for PSR J1841–0500 from Camilo et al. (2012), we find for this pulsar that the plasma density $\rho_{\text{plasma}} \simeq 400$ esu cm⁻³ is significantly larger than $\rho_{\text{GJ}} \simeq 130$ esu cm⁻³. The fact that these inferred densities all equal or exceed ρ_{GJ} at least implies that the basic conditions for radiation by the Goldreich & Julian (1969) model are being met.

For simplicity, the above calculations make the assumption that the pulsar is an orthogonal rotator. In reality, of course, the inclination angle between the spin and magnetic axes $\alpha < 90^\circ$. More recent and realistic modeling of the pulsar magnetosphere by Li et al. (2012) and Kalapotharakos et al. (2012) consider force-free electrodynamic and resistive solutions which can account for the different spin-down rates observed in these three intermittent pulsars. Based on our measurement of the on/off spindown ratio, \mathcal{R} , and the results presented in Fig. 3 of Li et al. (2012), the prediction for PSR J1832+0029 is that $\alpha \sim 60^\circ$. A future Arecibo observing campaign on this pulsar during its next on-state will be undertaken to obtain high-quality polarimetric data with the aim of constraining α . As discussed by Beskin & Nokhrina (2007) and Kalapotharakos et al. (2012), further discoveries of intermittent pulsars with different values of \mathcal{R} than observed so far would greatly help to constrain these models.

In the context of models for pulsar intermittency involving the neutron star’s emission mechanism, it should also be noted that Zhang, Gil & Dyks (2007) proposed that intermittent pulsars are old isolated neutron stars which have entered the so-called “death valley” in the $P - \dot{P}$ diagram (Chen & Ruderman 1993) where the voltage across the neutron star polar cap is no longer sufficient for pair production in the neutron star magnetosphere, and the radio emission becomes sporadic. Zhang et al. suggest that non-dipolar magnetic field

configurations, similar to the sunspot phenomenon, may be effective in such neutron stars and temporarily rejuvenate their radio emission. It is not clear, however, how the quasi-periodic nature seen in PSR B1931+24 can be explained quantitatively in this scenario, or indeed whether it applies to PSR J1832+0029 or PSR J1841–0500, since (as noted by Camilo et al. 2012) none of these pulsars are in the death valley region.

4.3. Constraints from the X-ray non-detections

The X-ray count rate upper limits can be used to estimate upper limits on energy flux, which, however, depend on assumed spectrum. We know from observations of old pulsars that their X-ray spectra can be approximated by an absorbed power-law model with a photon index $\Gamma \approx 2-4$ (e.g., Kargaltsev et al. 2006; Pavlov et al. 2009). The hydrogen column density toward the pulsar, $N_{\text{H}} \approx 1 \times 10^{21} \text{ cm}^{-2}$, can be estimated from the DM assuming a 10% average degree of ionization of the interstellar medium. Using the *Chandra* PIMMS tool⁴, we obtain the following absorbed and unabsorbed energy fluxes for a given source count rate R_s in the first observation: $F_{0.3-8 \text{ keV}}^{\text{abs}} = 0.63, 0.47$ and 0.48 , $F_{0.3-8 \text{ keV}}^{\text{unabs}} = 0.82, 0.90$ and 1.33 , in units of $10^{-15}(R_s/10^{-4} \text{ counts s}^{-1}) \text{ erg cm}^{-2} \text{ s}^{-1}$, for $\Gamma = 2, 3$ and 4 , respectively. For the second observation, the corresponding fluxes are $F_{0.3-8 \text{ keV}}^{\text{abs}} = 0.70, 0.55$ and 0.59 , $F_{0.3-8 \text{ keV}}^{\text{unabs}} = 0.91, 1.04$ and 1.64 , in the same units. Note that the same count rates correspond to higher fluxes in the second observation because the ACIS effective area became smaller. Using these relations and the count rate upper limits estimated above, we can estimate the flux upper limits at a given confidence level. For instance, for $\Gamma = 3$ and $C = 0.99$, we obtain $F_{0.3-8 \text{ keV}}^{\text{abs}} < 0.7$ and < 2.0 , $F_{0.3-8 \text{ keV}}^{\text{unabs}} < 1.3$ and < 3.8 , for the first and second observations, respectively, in units of $10^{-15} \text{ erg cm}^{-2} \text{ s}^{-1}$. From these upper limits, one can estimate upper limits on X-ray luminosity, $L_X = 4\pi d^2 F_X^{\text{unabs}}$ and efficiency, $\eta_X = L_X/\dot{E}$. For the on-state (where $\dot{E} = 4.0 \times 10^{32} \text{ erg s}^{-1}$), assuming $\Gamma = 3$, we obtain $L_{0.3-8 \text{ keV}} < 2.6 \times 10^{29}(d/1.3 \text{ kpc})^2 \text{ erg s}^{-1}$, $\eta_{0.3-8 \text{ keV}} < 6.5 \times 10^{-4}(d/1.3 \text{ kpc})^2$, at $C = 0.99$. Making the same assumptions for the off-state (where $\dot{E} = 2.4 \times 10^{32} \text{ erg s}^{-1}$), we obtain $L_{0.3-8 \text{ keV}} < 7.7 \times 10^{29}(d/1.3 \text{ kpc})^2 \text{ erg s}^{-1}$, $\eta_{0.3-8 \text{ keV}} < 3.0 \times 10^{-3}(d/1.3 \text{ kpc})^2$, at $C = 0.99$. These limits are consistent with the non-thermal efficiencies observed in other non-recycled pulsars (Possenti et al. 2002; Zavlin & Pavlov 2004).

⁴<http://asc.harvard.edu/toolkit/pimms.jsp>

4.4. Implications for other intermittency models

Our discussion so far has focused on pulsar intermittency as being due to processes that are internal to the neutron star magnetosphere. At least two alternative scenarios, which we discuss below, have been made to explain the phenomenon as being due to the influence of material emanating from outside the magnetosphere.

Cordes & Shannon (2008) investigated the consequences of debris disks around neutron stars, i.e. metal-rich leftover material from the supernova explosion that has aggregated into a disk of circumpulsar material. They propose a scenario in which the behavior seen in PSR B1931+24 is produced by an asteroid in an eccentric 40-day orbit which deflects material from the debris disk into the neutron star magnetosphere. Such a process could temporarily halt the electron-positron pair production thought to be responsible for the radio emission. Unfortunately, the infall rates required by this model translate to completely undetectable X-ray fluxes. In addition, given that sufficiently high-precision timing is not possible for pulsars such as PSR J1832+0029, any periodic signatures from such small bodies would not be detectable in its timing residuals (Fig. 3).

Rea et al. (2008) suggested that accretion onto the neutron star from a low-mass stellar companion in an eccentric orbit close to periastron could halt pair production. In this case, the heating of the infalling matter would produce additional X-rays in the off-state. While no signatures indicative of a binary companion exist in our radio timing residuals, such an orbit would not be detectable if it were close to face-on. Rea et al. attempted to test this hypothesis for PSR B1931+24 via a *Chandra* ACIS observation in 2006. Unfortunately, the pulsar switched on unexpectedly before their observations. To test this model in our observations of PSR J1832+0029, following the discussion in §5.2 from Rea et al. (2008), we assume that the radio emission is quenched when the neutron star’s Alfvén radius is less than its light cylinder radius. This corresponds to $L_X \gtrsim 10^{30} \text{ erg s}^{-1}$ and is right at the boundary of detectability in our off-state observation given the upper limit $L_{0.3-8 \text{ keV}} < 7.7 \times 10^{29} (d/1.3 \text{ kpc})^2 \text{ erg s}^{-1}$ found in §4.3. However, since the distance estimate to PSR J1832+0029 made using the Cordes & Lazio (2002) electron density model can be uncertain by factors of two or more (see, e.g., Deller et al. 2009) we cannot therefore conclusively reject this scenario as an explanation for the behavior observed in PSR J1832+0029.

4.5. How common are intermittent pulsars?

Regardless of the form of the mechanism for pulsar intermittency, its recognition and characterization through the three pulsars so far poses interesting questions as to the size of

the likely population of similar objects in the Galaxy. From our sampling of PSR J1832+0029 so far, it appears to spend approximately 50% of the time in the off-state. Similar considerations for PSRs B1931+24 and J1841–0500 imply similar off-state duty cycles. Due to these and similar pulsars being less likely to be on during pulsar search and confirmation observations, as noted by Kramer et al. (2006), they could represent a substantial population that has so far evaded detection. PSR J1841–0500, for example, was in an off-state during the closest PMPS observation, and was only discovered serendipitously during a search of a magnetar in the same telescope beam (Camilo et al. 2012). In addition to intermittent pulsars evading discovery in large-scale surveys, since a significant fraction of the ~ 1700 non-recycled pulsars currently known are not subject to long-term timing programs, it is currently unclear as to what fraction of these could exhibit intermittency on long time scales. Even the prototypical object B1931+24 evaded characterization for almost 20 years after its discovery (Stokes et al. 1985). For PSR J1832+0029, had the initial Parkes timing observations spanned a period of a year and no off-state seen, it is possible that the intermittent behavior would have evaded detection. Perhaps the majority of normal pulsars exhibit some form of intermittent behavior, if they are studied long enough. If that is the case, then current estimates of the pulsar birthrate would need to be upwardly revised by a factor of two. The impact of the discovery of intermittent pulsars on our understanding of the neutron star birth rate (see, e.g., Keane & Kramer 2008) is a currently unsolved problem which merits further investigation.

The Parkes radio telescope is part of the Australia Telescope, which is funded by the Commonwealth of Australia for operation as a National Facility managed by CSIRO. The Arecibo Observatory is operated by SRI International under a cooperative agreement with the National Science Foundation (AST-1100968), and in alliance with the Ana G. Méndez-Universidad Metropolitana, and the Universities Space Research Association. We thank Arun Venkataraman for retrieving the Arecibo observations. D.R.L., G.G.P., C.C., and M.A.M. were supported by *Chandra* grants GO8-9078 and GO1-12078 during part of this work. D.R.L. and M.A.M. were also supported by a WVEPSCoR Research Challenge Grant and acknowledge the support provided by the Australia Telescope National Facility distinguished visitor program during completion of this work. The work of G.G.P. was also partly supported by NASA grant NNX09AC84G and by the Ministry of Education and Science of Russian Federation (contract 11.G34.31.0001). We thank Fernando Camilo and Andrew Seymour for useful comments on the manuscript, as well as Christine Jordan for assistance with the Lovell timing data and George Hobbs for useful discussions concerning TEMPO2.

REFERENCES

- Backer, D. C. 1970, *Nature*, 228, 42
- Beskin, V. S., & Nokhrina, E. E. 2007, 308, 569
- Biggs, J. D. 1992, *ApJ*, 394, 574
- Camilo, F., Ransom, S. M., Chatterjee, S., Johnston, S., & Demorest, P. 2012, *ApJ*, 746, 63
- Chen, K., & Ruderman, M. 1993, *ApJ*, 408, 179
- Cordes, J. M., & Lazio, T. J. W. 2002, *astro-ph/0207156*
- Cordes, J. M., & Shannon, R. M. 2008, *ApJ*, 682, 1152
- Deller, A. T., Tingay, S. J., Bailes, M., & Reynolds, J. E. 2009, *ApJ*, 701, 1243
- Dowd, A., Sisk, W., & Hagen, J. 2000, in *Pulsar Astronomy - 2000 and Beyond*, IAU Colloquium 177, ed. M. Kramer, N. Wex, & R. Wielebinski (San Francisco: Astronomical Society of the Pacific), 275–276
- Espinoza, C. M., Lyne, A. G., Stappers, B. W., & Kramer, M. 2011, *MNRAS*, 414, 1679
- Gehrels, N. 1986, *ApJ*, 303, 336
- Goldreich, P., & Julian, W. H. 1969, *ApJ*, 157, 869
- Hobbs, G., Lyne, A. G., Kramer, M., Martin, C. E., & Jordan, C. 2004, *MNRAS*, 353, 1311
- Hobbs, G. B., Edwards, R. T., & Manchester, R. N. 2006, *MNRAS*, 369, 655
- Kalapotharakos, C., Kazanas, D., Harding, A., & Contopoulos, I. 2012, *ApJ*, 749, 2
- Kargaltsev, O., Pavlov, G. G., & Garmire, G. P. 2006, *ApJ*, 646, 1139
- Keane, E. F., & Kramer, M. 2008, *MNRAS*, 391, 2009
- Kramer, M. 2008, in *American Institute of Physics Conference Series*, Vol. 983, 40 Years of Pulsars: Millisecond Pulsars, Magnetars and More, ed. C. Bassa, Z. Wang, A. Cumming, & V. M. Kaspi, 11–19
- Kramer, M., Lyne, A. G., O’Brien, J. T., Jordan, C. A., & Lorimer, D. R. 2006, *Science*, 312, 549
- Li, J., Spitkovsky, A., & Tchekhovskoy, A. 2012, *ApJ*, 746, L24

- Lorimer, D. R., et al. 2006, MNRAS, 372, 777
- Lyne, A., Hobbs, G., Kramer, M., Stairs, I., & Stappers, B. 2010, Science, 329, 408
- Lyne, A. G. 2009, in Astrophysics and Space Science Library, Vol. 357, Astrophysics and Space Science Library, ed. W. Becker, 67
- Manchester, R. N., et al. 1996, MNRAS, 279, 1235
- . 2001, MNRAS, 328, 17
- McLaughlin, M. A., et al. 2006, Nature, 439, 817
- Pavlov, G. G., Kargaltsev, O., Wong, J. A., & Garmire, G. P. 2009, ApJ, 691, 458
- Possenti, A., Cerutti, R., Colpi, M., & Mereghetti, S. 2002, A&A, 387, 993
- Rankin, J. M. 1986, ApJ, 301, 901
- Rea, N., et al. 2008, MNRAS, 391, 663
- Ritchings, R. T. 1976, MNRAS, 176, 249
- Stokes, G. H., Taylor, J. H., Weisberg, J. M., & Dewey, R. J. 1985, Nature, 317, 787
- Wang, N., Manchester, R. N., & Johnston, S. 2007, MNRAS, 377, 1383
- Zavlin, V. E., & Pavlov, G. G. 2004, ApJ, 616, 452
- Zhang, B., Gil, J., & Dyks, J. 2007, MNRAS, 374, 1103

Table 1. Observed and derived parameters for PSR J1832+0029

Timing model parameters for first “on” period	
Data span (MJD)	52886 – 53152
Rotation frequency, ν (Hz)	1.87294940061(4)
Frequency derivative, $\dot{\nu}$ (10^{-15} s^{-2}) ..	–5.42(1)
Reference epoch (MJD)	53019
Timing model parameters for second “on” period	
Data span (MJD)	53796 – 55293
Right ascension, α (J2000)	18 ^h 32 ^m 50 ^s .825(1)
Declination, δ (J2000)	+00°29′27.0(3)
Rotation frequency, ν (Hz)	1.87294879924(1)
Frequency derivative, $\dot{\nu}$ (10^{-15} s^{-2}) ..	–5.44505(7)
Reference epoch (MJD)	54545
Timing model parameters for third “on” period	
Data span (MJD)	56128 – 56160
Rotation frequency, ν (Hz)	1.8729482220(8)
Frequency derivative, $\dot{\nu}$ (10^{-15} s^{-2}) ..	–5(2)
Reference epoch (MJD)	56144
Derived parameters for on-state	
Spin-down energy loss rate, $\dot{E} \propto \nu \dot{\nu}$.	$4.0 \times 10^{32} \text{ erg s}^{-1}$
Characteristic age, $\tau_c = \nu / (2 \dot{\nu})$	5.4 Myr
Surface magnetic field, $B \propto \sqrt{ \dot{\nu} /\nu^3}$	$9.2 \times 10^{11} \text{ G}$

Note. — Parentheses indicate 1- σ uncertainties on the last digit(s) as reported by TEMPO2.

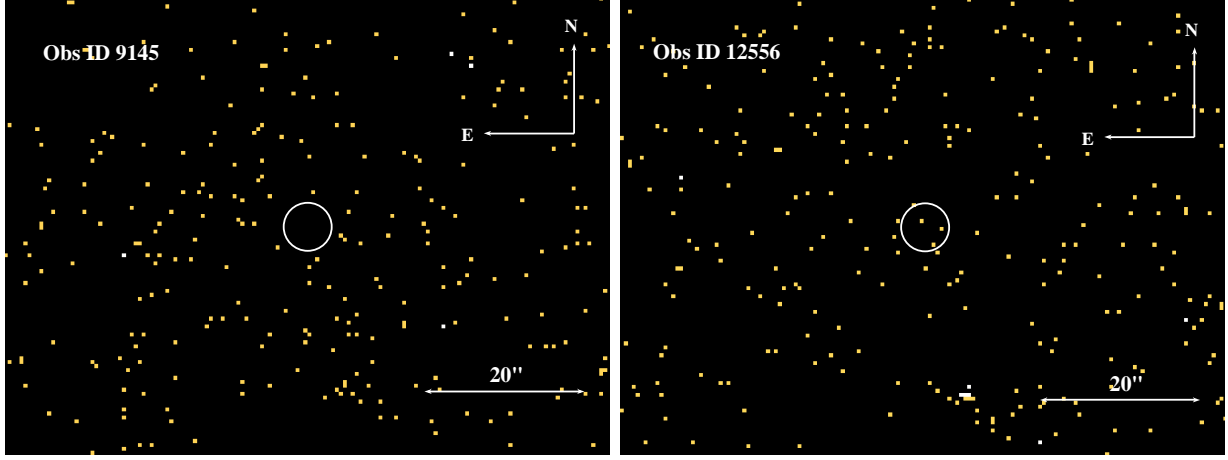


Fig. 1.— ACIS-S3 images of the PSR J1832+0029 field for the observations of 2007 October 19 (ObsID 9145) and 2011 March 28 (ObsID 12556), in the 0.3–8 keV band. The images have been corrected using astrometric measurements of 2MASS sources (see text). The $r = 3''$ circles are centered on the radio pulsar position from Table 1. The nearest detected X-ray object (barely seen in the first observation) is located $\approx 20''$ south of the pulsar.

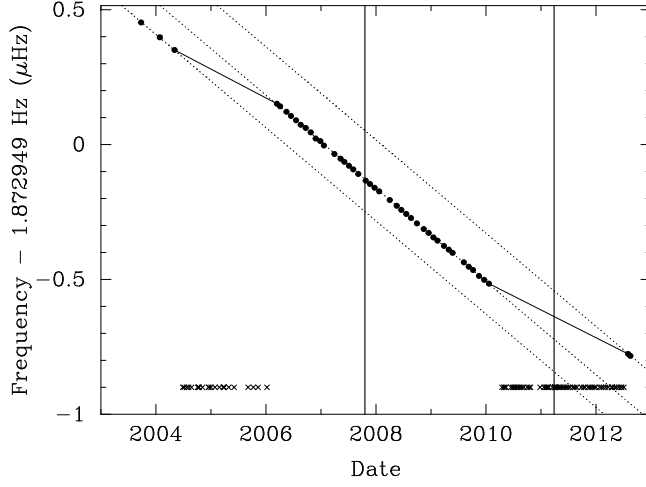


Fig. 2.— The rotational frequency history of PSR J1832+0029. The errors in the measurement of the data points are smaller than the size of the symbols. The three dotted lines show the $\dot{\nu}_{\text{on}}$ behavior as inferred from the TEMPO2 fit to the second on-state. The slanted solid lines show the frequency derivative inferred during the off-state. Epochs of non-detections in the Parkes and Jodrell timing campaigns are shown by the crosses. The vertical lines show the epochs of the two *Chandra* ACIS observations.

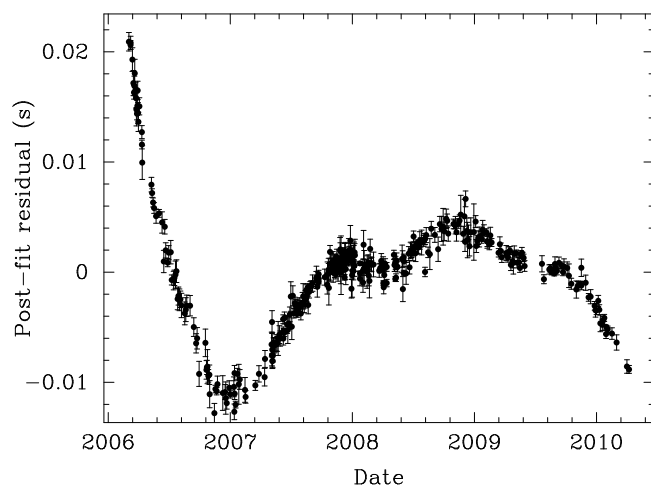


Fig. 3.— Timing model residuals for PSR J1832+0029 obtained from our TEMPO2 analysis of the second on-state using the ephemeris quoted in Table 1. The root-mean-square of the data shown here is 4.37 ms. These data, and all other pulse arrival times collected so far are freely available at <http://astro.phys.wvu.edu/J1832+0029>.